Pol. J. Environ. Stud. Vol. 26, No. 2 (2017), 925-933
DOI: *10.15244/pjoes/65470*

Original Research

Release Law of Sb, As, and Hg in Antimony Smelting Slag Under Simulated Acid Rain

Saijun Zhou*, Ning Li, Bozhi Ren, Peng Zhang

College of Civil Engineering, Hunan University of Science and Technology, Xiangtan 411201

Received: 26 June 2016
Accepted: 29 September 2016

Abstract

This study takes the Southern antimony smelting slag depot in Xikuangshan (XKS) Sb mine in the city of Lengshuijiang, Hunan, China, as the research object and explores the release law of Sb, As, and Hg in smelting slag under different pH-value simulated acid rain by a semi-dynamic leaching experiment of simulating the local rain. The results show that the leachate pH value is positively correlated with the pH value of simulated acid rain, while the leachate conductivity is negatively correlated with it. The leaching rates of As and Hg are negatively correlated with the pH value of the simulated acid rain, while the leaching rate of Sb is positively correlated with it; in the leaching process, the leachate pH value goes downward slowly after shooting up, but the leachate conductivity is continuously reduced; the releasing process of Sb, As, and Hg consists of two stages, and their leaching rate forms such an order as Sb > Hg > As. The diffraction peak intensity of the main mineral composition of quartz and calcite decreases significantly after leaching; the smelting slag's surface becomes less rough than before leaching, with fewer pores and edges, and the contents of S, Si, Al, Fe, Ca, and Sb on the slag surface decrease while the content of O, As, and Hg increases.

Keywords: antimony smelting slag, simulated rain, metal(loid)s, release law

Introduction

The exploitation and smelting of heavy metals causes serious environmental pollution, which has received extensive attention from researchers all over the world [1-3]. The smelting slag produced by the smelting mines is not only land-occupying, but also causes lasting environmental pollution, for large amounts of harmful elements in the smelting slag are released after rain [4-7]. As the world's largest antimony (Sb) producer, China produces on average 80% of global Sb annually [8]. Xikuangshan (XKS) in Hunan, the world's largest Sb mine, is reported to produce 25% of the world's total. The XKS mine has been mining and smelting for almost 120 years. Its longtime and large-scale mining and smelting has produced large amounts of smelting slag. With surface runoff and precipitation infiltration, harmful elements like Sb and the associated elements As and Hg have been released, threatening the environment and human beings [10-14]. When an excessive amount of Sb, As, or Hg enters the human body, it will cause diseases to the liver, skin, tumors, respiratory and cardiovascular systems, and even cancer [15-19]. Sb, As, Hg, and their compounds are listed as pollutants of priority interest by the United States

*e-mail: zsjaw0745@sina.com

Environmental Protection Agency [20] and the European Union [21].

Until the present, studies at home and abroad are mainly on minerals' adsorption of Sb (III and V) and its desorption, as well as Sb smelting slag's impact on the surrounding environment [22-27], but few are concerned with the precipitation of metal(loid)s from smelting slag under rainwater leaching, as well as their precipitation rule. Still less is the study on the precipitation characteristic and mechanism of metal(loid)s in Sb smelting slag. Therefore, this study takes Sb smelting slag in the XKS Sb mine as the research object and probes the precipitation characteristics and mechanism of such metal(loid)s as Sb, As, and Hg in Sb smelting slag by making a semi-dynamic leaching experiment of simulated local acid rain. It aims to provide theoretical support for the discharge and stockpiling of Sb smelting slag, metal(loid) pollution control, and environmental monitoring.

Material and Methods

Sample Collection

We collected the Sb smelting slag for our experiment from an open smelting slag yard near the southern XKS Sb mine in Lengshuijiang city, Hunan province (E111.4796°-E111.4835° and N27.7581°-27.7594°). The smelting slag yard covers an area of 22,000 m^2, with a stockpiling of about 30,000 tons of smelting slag. 20 sampling sites were selected around the slag yard with each sampling site being a square (1×1m). Each sample was a mixture of one-kilogram slag collected at the center and its four equidistant points of the sampling site, respectively, at the surface layer (0-30cm depth). The 20 samples were mixed uniformly, dried naturally, and then ground in a mill (XMQΦ240×90, Jiangxi Ganye, China) to make two kinds of samples with particle sizes less than 2 mm and 0.15 mm, respectively, for later use.

Test and Analysis Methods

Test Instrument and Reagent

The main test instruments include a DIYed semi-dynamic leaching device, consisting of a peristaltic pump, a leaching solution collection device, a leaching column (50 cm high and 5 cm in diameter; Fig. 1), AFS (Hydride Generation-Atomic Fluorescence Spectrometry, AFS-9700, Beingjing Haiguang, China), XRD (x-ray Diffraction, D8 Advance, Bruker AXS, Germany), SEM (scanning electron microscope, JSM-6380LV, JEOL, Japan), EDS (energy-dispersive spectrometry, GENESIS, EDAX, United States), oven (GZX-9246MBE, Shanghai Huyueming, China), pH meter (PB-10, Sartorius, Germany), conductivity meter (CCT-5320E, Hebei Ruida, China), and an ultrapure water machine (LBY-20, Chongqin Owen, China). The main reagents HNO_3, HF, and H_2O_2 (Sinopharm Chemical Reagent Co., Shanghai, China) are of super pure grade. Before use, all the vessels were soaked in 10% HNO_3 for 48 hours and rinsed with ultrapure water.

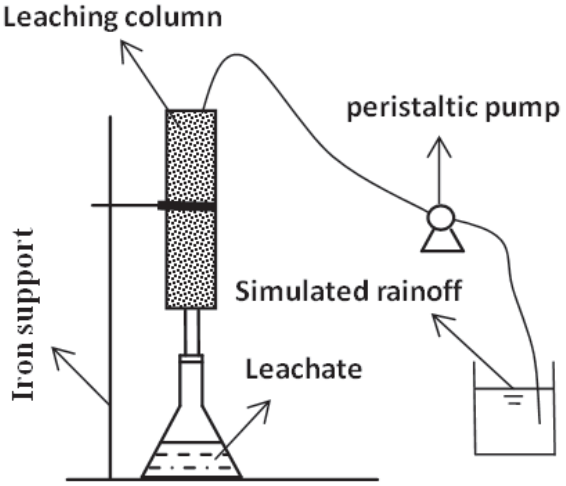

Fig. 1. Schematic diagram of leaching test device.

Basic Mineral Composition of Sb Smelting Slag and Trace Element Determination

The mineral composition of Sb smelting slag was observed and analyzed with XRD. The trace elements were determined by AFS (Sb, As, Hg, Pb, Cd, and Zn calibration curves showed good linearity: r>0.999) after the digestion of Sb smelting slag. The specific procedure is as follows: first, five samples of 0.1g smelting slag whose particle size is less than 0.15 mm and a blank sample were each put into a Teflon digestion tank; then, 5 ml of thick HNO_3 and 0.5 ml of HF were added into the tanks; next, the samples were put in an oven for digestion for 12 h at 170ºC; then after cooling, 1 ml of 30% H_2O_2 was added and 30 min later 10 ml of 5% HNO_3 was also added, and then the samples were filtered with a polyethylene film injection filter with an aperture of 0.2 μm. Finally, ultra-pure water was added to the samples to get a volume of 50 ml filtered fluid, respectively, and then kept at 4ºC. The content of trace elements was measured with AFS.

Trace elements exist in Sb smelting slag in various occurrence states, which exerts great influence on their precipitation during the semi-dynamic leaching process. This study adopts the improved extraction method [28] based on the sequential extraction method by Tessier [29] to extract occurrence states of Sb, As, and Hg in Sb smelting slag, and employs AFS to determine them.

Semi-dynamic Leaching Experiment of Sb Smelting Slag and Correlation Analysis

Under normal circumstances, the precipitation of inorganic pollutants in solid waste is mainly done through a static immersion test [30]. However, the fact is that solid waste is not completely soaked by water in most cases. Therefore, this study adopts a dry-wet alternate semi-

dynamic leaching experiment [5] to study the precipitation of such metal(loid)s as Sb, As, and Hg in Sb smelting slag.

Lengshuijiang city in Hunan province is the national sulfate acid rain control zone. The pH value of annual rainfall ranges from 4.06 to 6.36, with the weighted average pH of 4.98 [31]. Therefore, in this study rain can be simulated by a mixture of H_2SO_4 and HNO_3 solution at volumetric ratio of 3:1 and NaOH [32]. The simulated rain samples are of pH values 4.0, 5.0, and 6.0, respectively (hereinafter referred to as P4.0, P5.0, and P6.0). The mean monthly rainfall of the study area for each month from 1994 to 2013 was obtained from the Lengshuijiang Weather Bureau (Table 1), and simulated rain was prepared accordingly. Each leaching column was first loaded at the bottom with 5cm-thick quartz sand soaked by 5% HNO_3, above which two layers of filter paper were placed before the smelting slag (particle size less than 2mm) was put in. The column was then shaken to make the sample lay firm. 0.5L of ultrapure water was added to flow through a leaching column before the semi-dynamic leaching experiments to ensure that smelting slag was saturated. Then from the second day on, the simulated rain was allowed to flow through the leaching column at a rate of 50ml·h^{-1}, controlled by a peristaltic pump and then air dried. The process was repeated altogether 12 times, i.e., it experienced 12 times of half-day semi-dynamic leaching and 12 times of half-day dry (i.e, the 12-day simulation represents the rainfall of a year).

The leaching liquid was collected daily to determine conductivity and pH value; the content of Sb, As, and Hg in the leachate was determined by AFS. To ensure data accuracy, five parallel experiments were conducted for the samples, with each sample measured three times to get the average value. Comparison and analysis of antimony smelting slag samples before and after testing was conducted with XRD combined with SEM and EDS.

Quality Control

In order to ensure data accuracy in the analysis process and stability of test equipment, the standard reference soil (GBW07406) from China's National Institute of Metrology was treated in the same way as the slag samples, and the recovery rates of Sb, As, Hg, Pb, Cd, and Zn in standard reference materials are 95-106%, 94-107%, 94-104%, 97-105%, and 91-105%, respectively. At the same time, reagent blanks were added in each batch of analysis samples, and 20% of the samples were re-measured, with RSD (relative standard deviation) re-measurement less than 10%.

Results and Discussion

Content and Occurrence State of Metal(loid)s in Sb Smelting Slag

As shown in Table 2, the content of Sb and As in smelting slag is rather high, reaching 3,988.24 mg·kg^{-1} and 928.65 mg·kg^{-1}, respectively, being 1,338 and 66 times higher than the soil background values of heavy metals in Hunan Province [33]; although the Hg content is relatively lower (4.62 mg·kg^{-1}), it is still 51 times higher than the standard value. The amount of metal(loid)s in the samples shows great potential hazard.

The occurrence states of metal(loid)s Sb, As, and Hg in smelting slag before and after leaching are shown in Table 3. A comparison between the sum of the three elements in various occurrence states and the amount of elements in smelting slag indicates that the elements have high recovery rates after gradual extraction: the recovery rate of Sb before and after leaching is 90.69% and 89.03%, respectively; that of As is 86.64% and 86.62%, respectively; that of Hg is 92.86% and 92.79%, respectively. As for Sb distribution in various occurrence states before and after leaching, it forms the following order: residual fraction > organic and sulfide fraction > reducible fraction > carbonate fraction > exchangeable fraction. The amount of Sb in residual fraction before and after leaching accounts for 74.72% and 76.13%, respectively; As is mainly in the form of organic and sulfide fraction whether before or after leaching, accounting for 87.32% and 87.35%, respectively (and less in the form of reducible fraction and residual fraction, and least in the form of exchangeable fraction and carbonate fraction); Hg mainly exists in the form of residual fraction, accounting for 81.55% and 81.67% before and after

Table 2. Content and pollution levels of metal(loid)s in antimony smelting slag.

Element	Content (mg·kg^{-1})	Background value (mg·kg^{-1}) [33]	Excess multiple
Sb	3,988.24	2.98	1,338
As	928.65	14	66
Hg	4.62	0.09	51
Pb	59.18	27	2.2
Cd	1.61	0.079	20.4
Zn	778.57	95	8.2

Table 1. Annual rainfall distribution and corresponding simulated leaching amount (30% runoff was deleted).

Month	1	2	3	4	5	6	7	8	9	10	11	12
Depth (mm)	69.0	71.5	117.6	162.7	228.9	235.8	143.6	134.9	75.4	80.3	72.3	52.2
Volume (mL)	95	98	162	224	315	324	197	185	104	110	99	72

Table 3. Fraction analysis of metal(loid)s in antimony smelting slag.

Element		F1		F2		F3		F4		F5	
		Content mg·kg^{-1}	Proportion %	Content mg·kg^{-1}	Proportion %	Content mg·kg^{-1}	Proportion %	Content mg·kg^{-1}	Proportion %	Content mg·kg^{-1}	Proportion %
Before leaching	Sb	49.49	1.37	177.04	4.89	209.18	5.78	478.69	13.23	2702.67	74.72
	As	2.48	0.31	3.19	0.40	42.813	5.32	702.55	87.32	53.54	6.65
	Hg	0.042	0.98	0.369	8.61	0.173	4.03	0.207	4.83	3.497	81.55
After leaching	Sb	21.63	0.61	142.15	4.00	206.24	5.81	477.53	13.45	2703.26	76.13
	As	2.35	0.29	3.17	0.39	42.69	5.31	702.61	87.35	53.55	6.66
	Hg	0.036	0.84	0.368	8.58	0.174	4.06	0.208	4.85	3.501	81.67

Note: F1, exchangeable fraction; F2, carbonate fraction; F3, reducible fraction; F4, organic and sulfide fraction; F5, residual fraction.

leaching, respectively (less in carbonate fraction, organic and sulfide fraction, and reducible fraction, and least in exchangeable fraction, only accounting for 0.98% and 0.84% before and after leaching). It can be concluded from the above that the proportions of Sb, As, and Hg before and after leaching remains almost the same in their occurrence states, with changes only in carbonate fraction and exchangeable fraction.

Changing Rules of pH Values of Smelting Slag Leachate

Fig. 2 shows the pH changes of Sb smelting slag leachate under different pH-value simulated rain. As can be seen, the three samples are consistent in pH change trend in the whole process, all on the rise during the first six days; on the seventh day, the leachate pH values dropped to 8.24, 8.22, and 8.17, respectively; in the following five days, they remained basically stable, though with little ups and downs; to the twelfth day, they were 8.05, 8.17, and 8.21, respectively. During the whole leaching process, the leachate pH values formed such an order as P6.0>P5.0>P4.0. The leachate pH values influenced the metal(loid)s precipitation to an extent [34-35], which can also be proved by the precipitation rule of Sb, As, and Hg stated later in this paper.

The pH values of smelting slag leachate changed, which might result from the fact that the gangue minerals in antimony smelting slag are mainly alkaline minerals such as quartz and calcite, having a strong neutralizing ability [36]. Antimony ore became smelting slag with a layer of enamel surface structure after smelting, so during the first six days of leaching, the alkaline minerals in smelting slag were slowly released and reacted with H^+ in simulated rain, which made the pH value of leachate gradually increase. During the next six days, carbonate mineral in smelting slag was gradually reduced, as was the leachate pH value. As can be seen in Table 4, there exists in the smelting slag Al^{3+}, which may react with OH^- and then change into

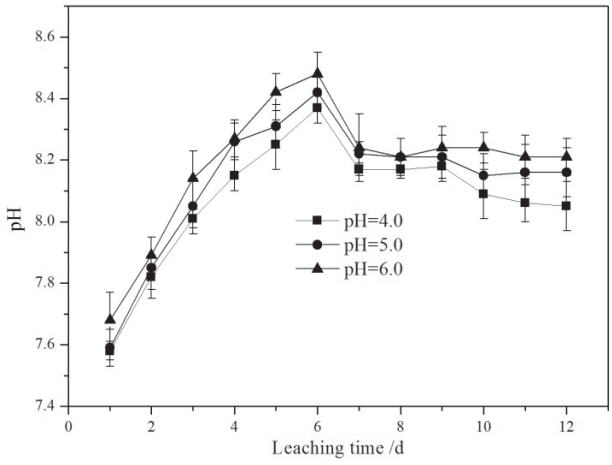

Fig. 2. Variation of pH value of leachate with leaching time under different simulated acid rains.

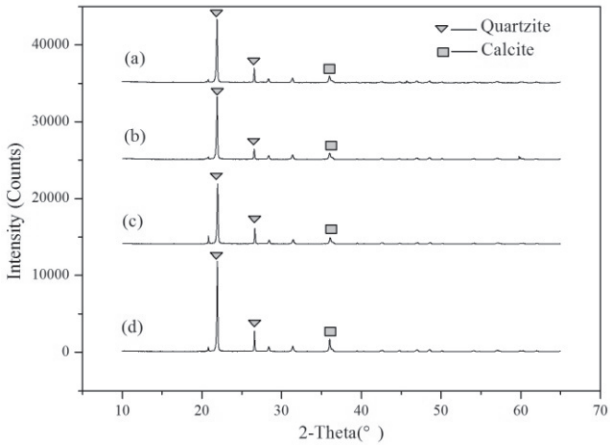

Fig. 3. XRD patterns on antimony smelting slags and different leaching residues at different pH: a) P4.0, b) P5.0, c) P6.0, and d) slag.

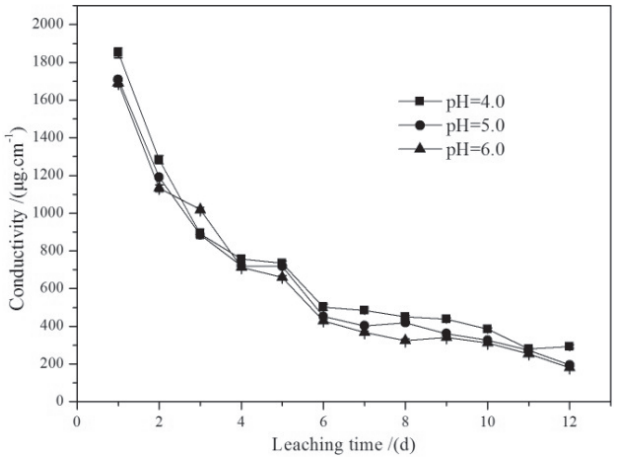

Fig. 4. Variations of conductivities of leachate with leaching time under different simulated acid rains.

$Al(OH)_3$. During the intervals of leaching, oxygen may react with the sulfide mineral (FeAsS) in the residue of smelting slag and generate H_2SO_4 and $Fe_2(SO4)_3$, which may in turn intensify the Oxidative dissolution of sulfide [37-38] and result in the reduction of leachate pH value.

Fig. 3(a-d) shows the XRD results of smelting slag samples leached through P4.0, P5.0, P6.0, and slag. On the axis of 2-Theta, the quartz diffraction peak appears at 21.9° and the calcite diffraction peak appears at 36.1°, which meets the study of relevant scholars [5]. The diffraction spectrums of the three samples are basically the same before and after leaching, but after leaching, the diffraction peak intensity of quartz and calcite significantly weakens. This may mean that quartz, calcite, and the metal(loid)s on the slag surface were partly released with the leachate.

Changing Rule of Leachate Conductivity

Fig. 4 shows the change of smelting slag leachate conductivity under different pH-value simulated acid rain. As can be seen, the conductivity of the three groups was gradually reduced with the increase of leaching time in the whole process; after leaching for 1 day, the leachate conductivities of P4.0, P5.0, and P6.0 were 1,850 $\mu s \cdot cm^{-1}$, 1,709 $\mu s \cdot cm^{-1}$, and 1,690 $\mu s \cdot cm^{-1}$, respectively; after leaching for 12 days, they fell to 292 $\mu s \cdot cm^{-1}$, 194 $\mu s \cdot cm^{-1}$, and 179 $\mu s \cdot cm^{-1}$, respectively. As can be seen from the curve, the conductivity basically formed such an order as P4.0> P5.0> P6.0 during the same leaching time, which means the lower the pH, the higher the conductivity of the leachate. In addition, with the leaching process going on, leachate conductivity declined, especially during the first four days of leaching, when it decreased significantly. During the last six days, leachate conductivity was reduced gently, which may be caused by the carbonate minerals (quartz and calcite) in smelting slag reacting intensely with H^+ in the leachate, and Na^+, K^+, Ca^{2+}, and Mg^{2+} on the surface of smelting slag quickly migrating to the leachate. The lower the pH in the leachate, the more rapid the reaction became and the greater the leachate conductivity. As the heavy metal ions and alkaline minerals on the surface of the smelting slag are washed out by the simulated acid rain in the early period, the alkaline minerals and heavy metal ions inside the smelting slag may release much more slowly in the late period. Besides, the migrated heavy metal ions may be adsorbed and precipitated. Therefore, leachate conductivity becomes weaker and weaker in the late period.

Release Law of Sb, As, and Hg from Smelting Slag

Fig. 5 shows the concentration change rule of Sb, As, and Hg in leachate under different pH simulated acid rain. As can be seen from Fig. 5 a), the change of leaching concentration of Sb in the leachate consists of two stages. In the initial stage of leaching (days 1-3), Sb concentration of the three samples reached the maximum rapidly, being 31.058 $mg \cdot L^{-1}$, 34.217 $mg \cdot L^{-1}$, and 42.025 $mg \cdot L^{-1}$, respectively. This may be because after the first three days of leaching, the enamel surface structure of smelting slag was destroyed and stibnite (Sb_2S_3) was oxidized to SbO_3^{-1} in the oxygen-enriched environment to the leachate [39]. The specific reaction is as follows:

$$Sb_2S_3 + 3H_2O + 6O_2 = 3SO_4^{2-} + Sb_2O_3 + 6H^+ \quad (1)$$

$$Sb_2O_3 + 3H_2O = 2SbO_3^- + 6H^+ + 4e \quad (2)$$

During the period from days 4 to 12, because of the neutralizing reaction of the carbonate minerals the leachate was weakly alkaline, and there was a certain amount of OH^- in the solution, which may react with Al^{3+} and Fe^{3+} in the leachate, generating gels like $Al(OH)_3$ and $Fe(OH)_3$, which formed a thin film covering the smelting slag surface to prevent further oxidation of stibnite. Moreover, as can be seen from Fig. 5a), Sb concentration and pH

value in simulated rain leaching are inversely proportional, and this may be due to Sb's double characteristics: Sb in the smelting slag turned into SbO_3^{-1} during the leaching process and then turned into deposit $Sb(OH)_5$, which under higher pH value formed soluble Sb $(OH)_6^{-1}$ [40]. After 12 days of leaching, Sb concentrations of the three samples were 19.687 mg·L^{-1}, 20.199 mg·L^{-1}, and 22.776 mg·L^{-1}, respectively.

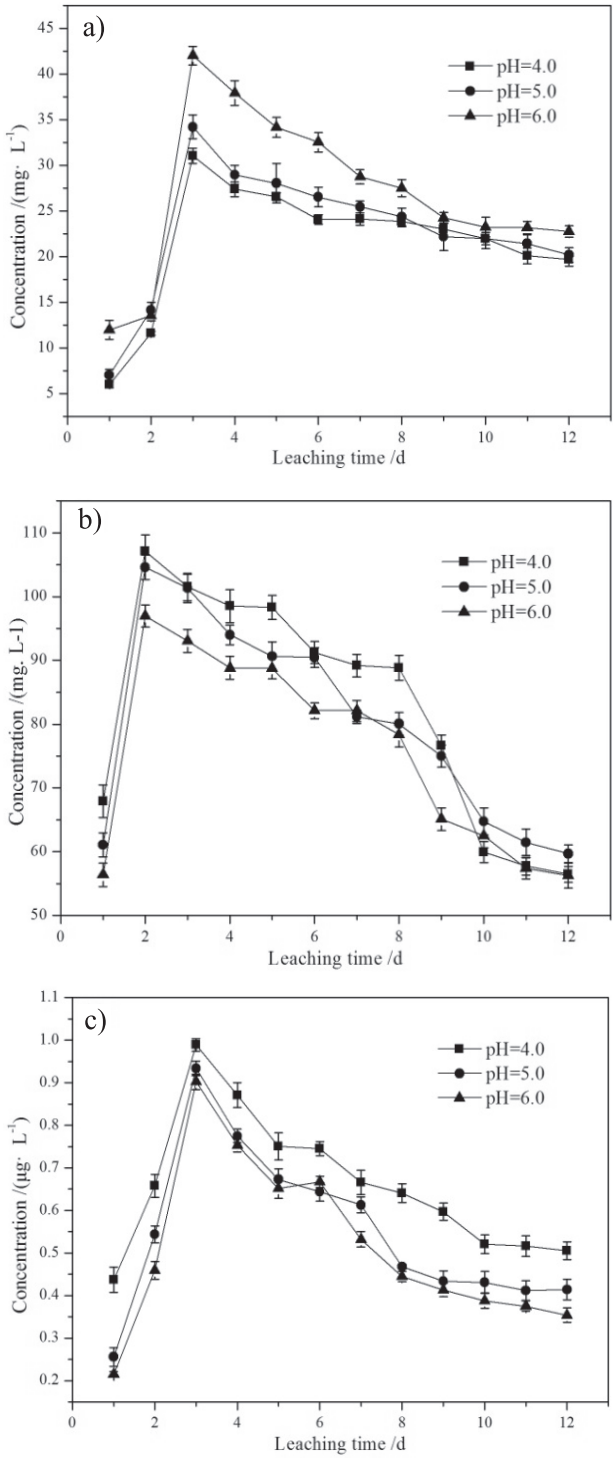

Fig. 5. Variations of a) Sb, b) As, and c) Hg concentrations in leachate with leaching times under different simulated acid rains.

Fig. 5 (b, c) show that the concentrations of As and Hg in leachate were consistent in changing trend with the leaching time going. After two days of leaching, As concentration in P4.0, P5.0, and P6 leachate reached maximums of 96.973 μg·L^{-1}, 104.608 μg·L^{-1}, and 107.097 μg·L^{-1}, respectively, while Hg concentrations in P4.0, P5.0, and P6.0 leachate reached their respective maximums in three days: 0.902 μg·L^{-1}, 0.934 μg·L^{-1}, and 0.989 μg·L^{-1}. The main reason may be that As and Hg in exchangeable fraction can be easily oxidized and then dissolved into leachate [41-42]. The specific reaction is as follows:

$$FeAsS + 11Fe^{3+} + 7H_2O = 12Fe^{2+} + H_3AsO_4 + 11H^+ + SO_4^{2-} \quad (3)$$

$$HgS + 2O_2 = Hg^{2+} + SO_4^{2-} \quad (4)$$

The concentrations of As and Hg in the leaching began to fall from days 3 and 4, respectively, which may be caused by that with As and Hg in exchangeable fraction having released mostly in the early days, As and Hg in other forms just released slightly, and had little effect on As and Hg concentration in the leachate. In addition, with the leaching going, the generated AsO_4^{3-} can be easily absorbed by gels like $Al(OH)_3$ and $Fe(OH)_3$, and the generated Hg^{2+} can be easily absorbed by calcite.

Fig. 6 shows the accumulated release amount of metal(loid)s Sb, As, and Hg in smelting slag under acid rain of different pH values. As shown in Fig. 6, the release amount of Sb, As, and Hg in 0.5kg Sb smelting slag under simulated rain of different pH values after 12 days were respectively in the range of 46.618~55.516 μg, 148.918~164.120 μg, and 1.072~1.314 μg, and the heavy metal leaching rate (heavy metal leaching rate = accumulated release amount of heavy metals/amount of heavy metals) under simulated rainfalls of different pH values were in the range of 2.345~2.792%, 0.016~0.018%, and 0.018~0.028%, respectively. The release rate of

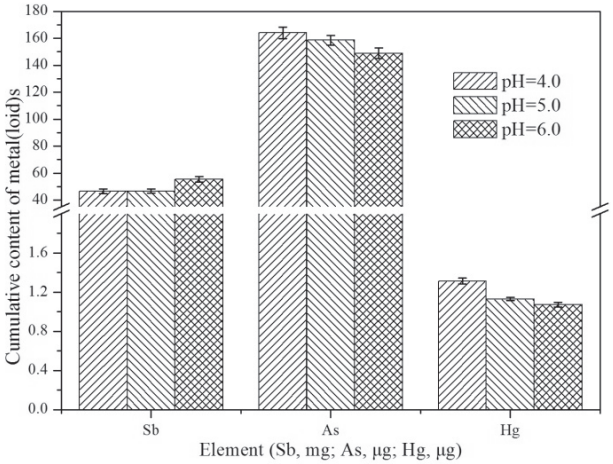

Fig. 6. Cumulative contents of different metal(loid)s.

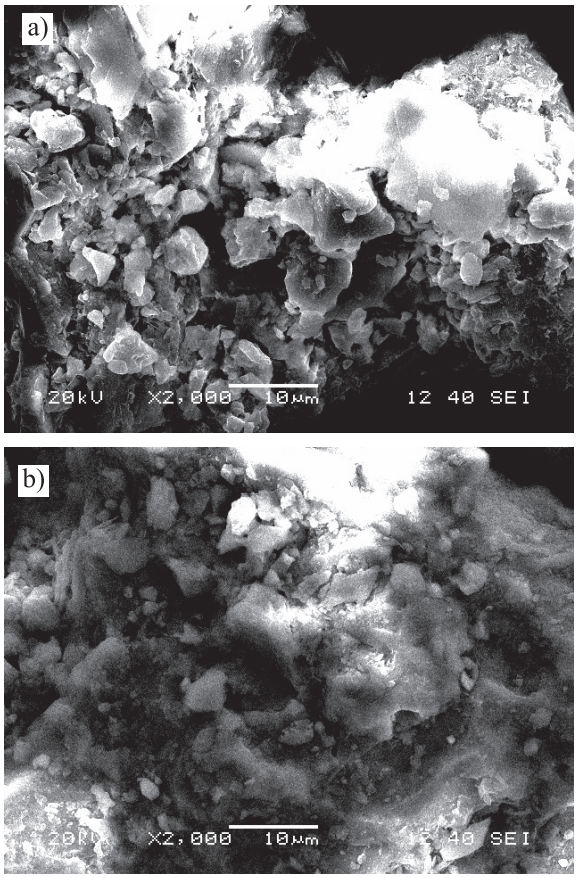

Fig. 7. SEM images of antimony smelting slag before and after leaching: a) before leaching, b) after leaching.

different metal(loid)s in Sb smelting slag is different, following the order Sb > Hg > As. The reasons may be as follows: first, the metal(loid)s content in smelting slag is different; second, it is associated with the characteristics and the existing forms of metal(loid) ions.

Table 3 shows that Sb and Hg are mainly in the state of residue, accounting for 74.72% and 81.55%, respectively, and As is mainly in exchangeable fraction, accounting for 87.32%; Sb, As, and Hg are least in exchangeable fraction, accounting for only 1.37%, 0.31%, and 0.98%, respectively. Therefore, the leaching rate of Sb, Hg, and As in the smelting slag decreased in turn. In addition, as Fig. 5 shows, the leaching rate of As and Hg under simulated rains formed such an order as P4.0 >P5.0> P6.0, which indicated that the lower the pH value, the higher the leaching rate As and Hg; Sb leaching rate in P4.0 and P5.0 shared little difference while it was much higher under P6.0.

Analysis of SEM Test

Sample P6.0 was selected for morphology analysis before and after leaching. Its SEM images of smelting slag surface before and after leaching for 12 days are shown in Fig. 7. As can be seen, its morphology has changed significantly. Before leaching, the slag surface was rough, with more pores and edges; after leaching for 12 days, it became slightly broken, but seemed less rough. The contrast of smelting slag's stomatal morphology shows that the smelting slag surface had fewer pores after leaching. This may be due to the minerals on the slag surface having migrated to the leachate under leaching, erosion, and Redox reaction of simulated acid rain. In addition, during the period of leaching, some ions were precipitated and absorbed by the slag surface, so some of the pores had been blocked.

Analysis of EDS Test

Sample P6.0 is taken for EDS analysis to explore the transfer rule of the metal(loid)s in Sb smelting slag, both before and after leaching. The results are shown in Table 4. As can be seen, before leaching the main compositions in smelting slag are O, Si, Al, and Fe; after leaching, the content of S, Si, Al, Fe, Ca, and Sb was reduced, while the contents of O, As, and Hg increased; the reduction of S, Si, Al, Fe, Ca, and Sb indicates that a large number of them migrated into the leachate under the effect of erosion of simulated acid rain and oxidation; the increase of O may be caused by the metal(loid)s on the slag surface being precipitated under leaching, and adsorbed on the slag surface in the forms of metal hydroxide and metal complex [43-44]; the increase of As and Hg may result from the exposure of inside-slag As and Hg under leaching.

Conclusion

The contents of Sb, As, and Hg in the Sb smelting slag in XKS Mine reach 3,988.24 mg·kg^{-1}, 4.62 mg·kg^{-1}, and 928.65 mg·kg^{-1}, respectively, making it 1,388, 66, and 51 times higher, respectively, than the soil background values of heavy metals in Hunan Province. This causes potential danger to the mining area. The smelting slag is under leaching treatment with simulated acid rains of various pH values; leachate pH value, leachate conductivity, accumulated release quantity, and release rate of Sb, As, and Hg all show certain relevance with the pH values of the acid rain. The smaller the pH value, the smaller

Table 4. Main elements on slag surface before and after leaching by EDS (%, mass fraction).

	O	Si	Al	Fe	Ca	S	Pb	Cd	Cu	Mn	K	Cr	Sb	As	Hg
Before leaching	45.31	43.79	2.71	2.02	1.27	1.46	1.23	0.08	0.45	0.33	0.25	0.02	1.02	0	0.06
After leaching	52.77	40.23	1.25	0.58	0.65	1.12	1.02	0.06	0.12	0.17	0.02	0.31	0.69	0.57	0.44

the leachate pH value and the greater the leachate's conductivity, the greater the accumulated release quantity and the release rate of As and Hg, but the smaller the accumulated release quantity and release rate of Sb.

As regards the leaching process of smelting slag, there are two stages for the leaching of the metal(loid)s Sb, As, and Hg, namely in the first stage, the leaching develops rapidly and in the second stage it leaches slowly. Sb and Hg leaching reaches the maximum leaching concentration in three days, while As reaches its maximum leaching concentration in two days. The maximum values of the leaching rate of Sb, As, and Hg are 2.792%, 0.018%, and 0.028%, respectively. Under different acid rains, the leaching rates of Sb, As, and Hg forms such an order as Sb > Hg > As.

The XRD analysis of Sb smelting slags shows that the main minerals in the sample are quartz and calcite, and their diffraction peak intensity decreases significantly after the leaching of simulated acid rain. SEM and EDS analysis shows that the smelting slag surface becomes less rough, with fewer pores and edges. After 12 days of leaching, S, Si, Ca, Sb, Fe, and Hg on the slag surface decrease, while O, As, and Hg increase.

Acknowledgements

This research was financially supported by the National Natural Science Foundation of China (No. 42472328) and the Ministry of Education in China Project of Humanities and Social Science (Nos. 13YJCZH276 and 14YJA630039).

References

1. KAPUSTA P., SOBCZYK Ł. Effects of heavy metal pollution from mining and smelting on enchytraeid communities under different land management and soil conditions. Sci. Total Environ., **536**, 517, **2015**.
2. ESCARRÉ J., LEFÈBVRE C., RABOYEAU S., DOSSANTOS A., GRUBER W., MAREL J.C.C., FRÉROT H., NORET N., MAHIEU S., COLLIN C., OORT F.V. Heavy Metal Concentration Survey in Soils and Plants of the Les Malines Mining District (Southern France): Implications for Soil Restoration. Water Air and Soil Poll., **216**, 485, **2011**.
3. ASENSIO V., VEGA F.A., SINGH B.R., COVELO E.F. Effects of tree vegetation and waste amendments on the fractionation of Cr, Cu, Ni, Pb and Zn in polluted mine soils. Sci. Total Environ., **443**, 446, **2013**.
4. VÍTKOVÁ M., ETTLER V., MIHALJEVIČ M., ŠEBEK O. Effect of sample preparation on contaminant leaching from copper smelting slag. J. Hazard. Mater., **197**, 417, **2011**.
5. LI H.B., WANG Z.X., YANG Z.H., CHAI L.Y., LIAO Y.P. Static and Dynamic leaching of chromium(VI) from chromium-containing slag. Environ. Eng Sci., **29**, 426, **2012**.
6. COSTA A G., POLETTINI B A., POMI B R., STRAMAZZO B A. Leaching modelling of slurry-phase carbonated steel slag. J. Hazard. Mater., **302**, 415, **2016**.
7. POTYSZ A., KIERCZAK J., FUCHS Y., GRYBOS M., GUIBAUD G., LENS P.N.L., HULLEBUSCH E.D.V. Characterization and pH-dependent leaching behaviour of historical and modern copper slags. J. Geochem. Explor., **160**, 1, **2016**.
8. U.S. Geological Survey, Mineral Commodity Summaries 2013., Washington, **2013**.
9. TAO Y., JIN J.F. Paragenesis and differentiation of As, Au with Sb in Xikangshan-type antimony deposits, Central Hunan. Acta mineralogical sincia, **21**, 67, **2001** [In Chinese].
10. HE M.C. Distribution and phytoavailability of antimony at an antimony mining and smelting area, Hunan, China. Environ. Geochem. Hlth., **29**, 209, **2007**.
11. WANG X.Q., HE M.C., XIE J., XI J.H., LU X.F. Heavy metal pollution of the world largest antimony mine-affected agricultural soils in Hunan province (China). J. Soil. Sediment., **10**, 827, **2010**.
12. OKKENHAUG G., ZHU Y.G., LUO L., LEI M., LI X., MULDER J. Distribution, speciation and availability of antimony (Sb) in soils and terrestrial plants from an active Sb mining area. Environ Pollut., **159**, 2427, **2011**.
13. ZENG D.F., ZHOU S.J., REN B.Z., CHEN T.S. Bioaccumulation of antimony and arsenic in vegetables and health risk assessment in the superlarge antimony-mining area, China. J. Anal Methods Chem., Article ID 909724, 9 pages. Volume **2015**.
14. WEI C.Y., GE Z.F., CHU W.S., FENG R.W. Speciation of antimony and arsenic in the soils and plants in an old antimony mine. Environ. Exp. Bot ., **109**, 31, **2015**.
15. KURODA K., ENDO G., OKAMOTO A., YOO Y., HORIGUCHI S. Genotoxicity of beryllium, gallium and antimony in short-term assays. Mutat. Res., **264**, 163, **1991**.
16. SCHNORR T.M., STEENLAND K., THUN M.J., RINSKY R.A. Mortality in a cohort of antimony smelter workers. Am. J. Ind. Med., **27**, 759, **1995**.
17. STATES J.C., SRIVASTAVA S., CHEN Y., BARCHOWSKY A. Arsenic and cardiovascular disease. Toxicol. Sci., **107**, 312, **2009**.
18. PARVEZ F., CHEN Y., BRANDT-RAUF P.W., BERNARD A., DUMONT X., SLAVKOVICH V., ARGOS M., D'ARMIENTO J., FORONJY R., HASAN M.R., EUNUS H.E., GRAZIANO J.H., AHSAN H. Nonmalignant respiratory effects of chronic arsenic exposure from drinking water among never-smokers in Bangladesh, Environ. Health Perspect. **116**, 190, **2008**.
19. NORDBERG G. Handbook on the Toxicology of Metals, Academic Press, Amsterdam, Boston, **2007**.
20. USEPA. Water Related Fate of the 129 Priority Pollutants, WASHINGTON D.C., **1979**.
21. European Council. Directive 76/464/EEC-Water pollution by discharges of certain dangerous substance. **1976**.
22. FLYNN H.C., MEHARG A.A., BOWYER P.K., PATON G.I. Antimony bioavailability in mine soils. Environ Pollut., **124**, 93, **2003**.
23. CIDU R., BIDDAU R., DORE E., VACCA A., MARINI L. Antimony in the soil-water-plant system at the Su Suergiu abandoned mine (Sardinia, Italy): Strategies to mitigate contamination. Sci. Total Environ.,497-498, 331, **2014**.
24. WANG X.Q., HE M.C., XI J.H., LU X.F. Antimony distribution and mobility in rivers around the world's largest antimony mine of Xikuangshan, Hunan Province, China. Microchem J., **97**, 4, **2011**.
25. TIGHE M., LOCKWOOD P., WILSON S. Adsorption of antimony(V) by floodplain soils, amorphous iron(III) hydroxide and humic acid. J. Environ. Monit., **7**, 1177, **2005**.
26. LEUZ A.K., MÖNCH H., JOHNSON C.A. Sorption of Sb(III) and Sb(V) to goethite: influence on Sb(III) oxidation and mobilization. Environ. Sci. Technol., **40**, 7277, **2006**.

27. MITSUNOBU S., MURAMATSU C., WATANABE K., SAKATA M. Behavior of antimony(V) during the transformation of ferrihydrite and its environmental implications. Environ. Sci. Technol., **47**, 9660, **2013**.
28. LEE P.K., YU S.Y. Lead isotopes combined with a sequential extraction procedure for source apportionment in the dry deposition of Asian dust and non-Asian dust. Environ Pollut., **210**, 65, **2016**.
29. TESSIER A., CAMPBELL P.G.C., BISSION M. Sequential extraction procedure for the speciation of particulate trace metals. Anal Chem., **51**, 844, **1979**.
30. KOSSON D.S., VAN DER SLOOT H.A., and EIGHMY T.T. An approach for estimation of contaminant release during utilization and disposal of municipal waste combustion residues. J. Hazard. Mater., **47**, 43, **1996**.
31. Environmental protection bureau of Loudi city. Bulletin of the environmental situation of Loudi city. **2014** [In Chinese].
32. ZHANG G., ZENG G.M., JIANG Y.M., LIU H.L. Analysis on the variant characteristics, present situation and origin of acid rain in Hunan Province. Res. Environ Sci., **16**, 14, **2003** [In Chinese].
33. PAN Y., YANG G. Background value of soils in Hunan and their investigation methods. China Environmental Science Press, **1988** [In Chinese].
34. LIANG B., ZHENG X.Z., JIN J.X., BAI Y.P. Influence of acid and alkali solutions leaching on the water and heavy metal contents of tail ore. Journal of Guangxi University, **37**, 539, **2012** [In Chinese].
35. POTYSZ A., KIERCZAK J., Fuchs Y., GRYBOS M., GUIBAUD G., LENS P.N.L., HULLEBUSCH E.D.V. Characterization and pH-dependent leaching behavior of historical and modern copper slags. J. Geochem. Explor., **160**, 1, **2016**.
36. PAKTUNC A.D. Mineralogical constraints on the determination of neutralization potential and prediction of acid mine drainage. Environ. Geo., **39**, 103, **1999**.
37. DUTRIZAC J.E. The dissolution of sphalerite in ferric sulfate media. Metall Mater Trans. B., **37**, 171 , **2006**.
38. SOUZA A.D., PINA P.S., LEÃO V.A., SILVA C.A., SIQEIRA P.F. The leaching kinetics of a zinc sulphide concentrate in acid ferric sulphate. Hydrometallurgy, **89**, 72, **2007**.
39. ASHLEY P.M., CRAW D., GRAHAM B.P., CHAPPELL D.A. Environmental mobility of antimony around mesothermal stibnite deposits, New South Wales, Australia and New Zealand. J. Geochem Exp., **77**, 1, **2003**.
40. ZHU J., WU F.C. Treatment of wastewater released from antimony ore processing using acidified coal fly ash. Acta Sci. Circumst., **30**, 361, **2010** [In Chinese].
41. YU Y., ZHU Y., GAO Z., GAMMONS C.H., LI D. Rate of arsenopyrite oxidation by oxygen and Fe(III) at pH 1.8-12.6 and 15-45ºC. Environ. Sci. Technol., **41**, 6460, **2007**.
42. ZHANG G.P., LIU C.Q., WU P., YANG Y.G. Environmental geochemical characteristics of mine wastes from the Wanshan mercury mine, Guizhou, China. Acta Mieralogica Sinica, **24**, 231, **2004** [In Chinese].
43. MARX S.K., LAVIN K.S., HAGEMAN K.J., KAMBER B.S., O'LOINGSIGH T., MCTAINSH G.H. Trace elements and metal pollution in aerosols at an alpine site, New Zealand: Sources, concentration and implications. Atmos Environ., **82**, 206, **2014**.
44. SAIKIA B.K., WARD C.R., OLIVEIRA M.L.S., HOWER J.C., LEAO F.D., JOHNSTON M.N., O'BRYAN A., SHARMA A., BARUAH B.P., SILVA L.F.O. Geochemistry and nano-mineralogy of feed coals, mine overburden, and coal-derived fly ashes from Assam (North-east India): a multi-faceted analytical approach. Int J. Coal Geol. **137** ,19, **2015**.